

# Supplementary Information for: Breaking the Electrical Barrier between Copper and Carbon Nanotubes

Karolina Z. Milowska,<sup>\*,†</sup> Mahdi Ghorbani-Asl,<sup>\*,†,‡</sup> Marek Burda,<sup>†</sup> Lidia  
Wolanicka,<sup>†</sup> Nordin Ćatić,<sup>†</sup> Paul D. Bristowe,<sup>†</sup> and Krzysztof K. K. Koziol<sup>\*,†,¶</sup>

<sup>†</sup>*Department of Materials Science and Metallurgy, University of Cambridge, 27 Charles  
Babbage Rd, CB3 0FS Cambridge, United Kingdom*

<sup>‡</sup>*Institute of Ion Beam Physics and Materials Research, Helmholtz-Zentrum  
Dresden-Rossendorf, 01314 Dresden, Germany*

<sup>¶</sup>*Current address: Cranfield University, School of Aerospace, Transport and  
Manufacturing, Building 61, Cranfield, Bedfordshire, MK43 0AL, United Kingdom*

E-mail: karolina.milowska@gmail.com; mahdi.ghorbani@hzdr.de; k.koziol@cranfield.ac.uk

Phone: +44(0) 1234 754038

# Geometry Optimization

The part of the composite model labelled  $t$  in Fig.1 (d) was fully optimized using 3D periodic boundary conditions with a maximum force tolerance equal to  $0.01 \text{ eV}/\text{\AA}$ . The interface areas (labelled  $i$ ) were subjected to a more standard optimization procedure using a force convergence criterion of  $0.15 \text{ eV}/\text{\AA}$ . The total energy tolerance criterion ( $10^{-4} \text{ eV}$ ) remained the same during all optimization steps.

## Structural, Energetic and Electrostatic Properties

The distortion of the CNT due to the surrounding Cu matrix and alloying elements is quantified using the coefficient of variation of the CNT radius, CV, which is defined as the ratio of the standard deviation to the mean of the CNT radius.<sup>1</sup> The mechanical stability of a Cu-M-CNT composite is assessed using the interfacial strength  $\tau$  and matrix internal surface energy  $\gamma$ . The interfacial strength is defined as:

$$\tau = -\frac{E_{comp} - E_{matrix} - E_{CNT}}{A_{int}}, \quad (1)$$

where  $E_{matrix}$ ,  $E_{CNT}$  and  $E_{comp}$  are the total energies of the metal matrix, CNT and composite, respectively. The interfacial area,  $A_{int}$ , is the sum of the lateral surface area of the CNT ( $(2\pi(\bar{r} + t)l)$ ) and its two end areas ( $4\pi(\bar{r}_l + \bar{r}_r)t$ ). The average radius of the CNT ( $\bar{r}$ ) was determined as a geometric average of distances between the axis of the tube and all carbon atom positions, whereas the radius of the left(right) end ( $r_{l(r)}$ ) of the tube takes into account only the position of C atoms at the left(right) end. The thickness of the CNT,  $t$ , is equal to  $2r_C$ , where  $r_C$  is the van der Waals radius of a carbon atom ( $1.7 \text{ \AA}$ ).

The matrix internal surface energy is defined as:

$$\gamma = -\frac{E_{matrix} - \sum_{\alpha=1}^N E_{atom,\alpha}}{A_{cavity}}, \quad (2)$$

where  $A_{cavity}$  is the internal surface of the matrix cavity formed by the CNT and  $E_{(atom,\alpha)}$  is the total atomic energy of a bulk atom of type  $\alpha$  (Cu, Ni, Cr, or Al).

The electrostatic difference potential was calculated as the difference between the electrostatic potential of the self consistent valence charge density and the electrostatic potential from a superposition of atomic valence densities.

## Transport Properties

The transmission coefficients,  $T(\epsilon, U)$ , of electrons with energy  $\epsilon$  incident in the central scattering region constituting the device under a bias voltage  $U$ , was calculated using the following expression:

$$T(\epsilon, U) = G(\epsilon)\Gamma_l G^\dagger(\epsilon)\Gamma_r, \quad (3)$$

where  $G(\epsilon)$  is the Green's function of the central region and  $\Gamma_{l(r)}$  is a matrix accounting for the coupling of the central region to the left (right) electrode. Consequently, the conductance can be expressed as follows:

$$G(\epsilon) = G_o Tr[T(\epsilon, U)], \quad (4)$$

where  $G_o = 2e^2/h$  is the unit of quantum conductance. The discrepancy between the theoretical and experimental conductance can be attributed to inelastic effects which are not taken into account in this method.

The electrical current through the device under non-equilibrium conditions, i.e. under a finite bias voltage,  $U$ , was calculated using the Landauer-Büttiker formula:

$$I(U) = \frac{2e}{h} \int_{-\infty}^{+\infty} T(\epsilon, U) (f_l(\epsilon - \mu_l) - f_r(\epsilon - \mu_r)) d\epsilon, \quad (5)$$

where  $\mu_{l(r)} = E_F \pm eU/2$  is the electrochemical potential of the left (right) electrode, and  $f_{l(r)}$  is the corresponding Fermi-Dirac electron distribution.  $E_F$  is the Fermi energy.

The current density,  $j$ , was calculated as a ratio of the electrical current  $I$ , to the average cross-sectional area  $\bar{A} = V/l_c$ , where  $V$  is the volume of a system and  $l_c$  is the  $z$ -dimension of the model.

Spin polarization only has a significant impact on the transport properties of Cu-Cr-CNT systems. Due to computational constraints, spin-orbit coupling was only assessed for the carpet systems. It was found to have a negligible impact on their transport properties.

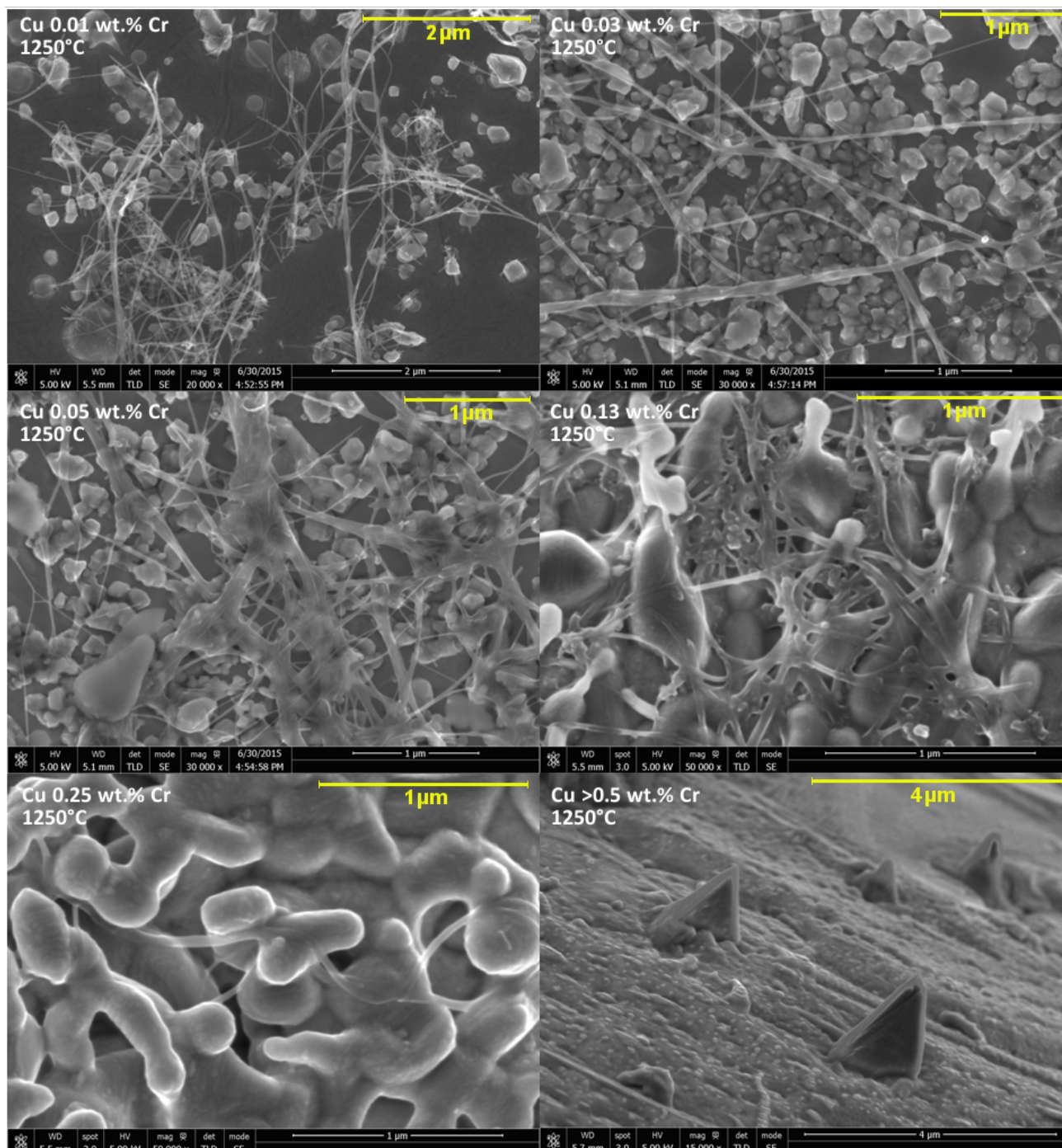


Figure S1: SEM images of cross-sections through several Cu-Cr-CNT composites having different Cr concentrations after vacuum heat-treatment of up to 1250° C.

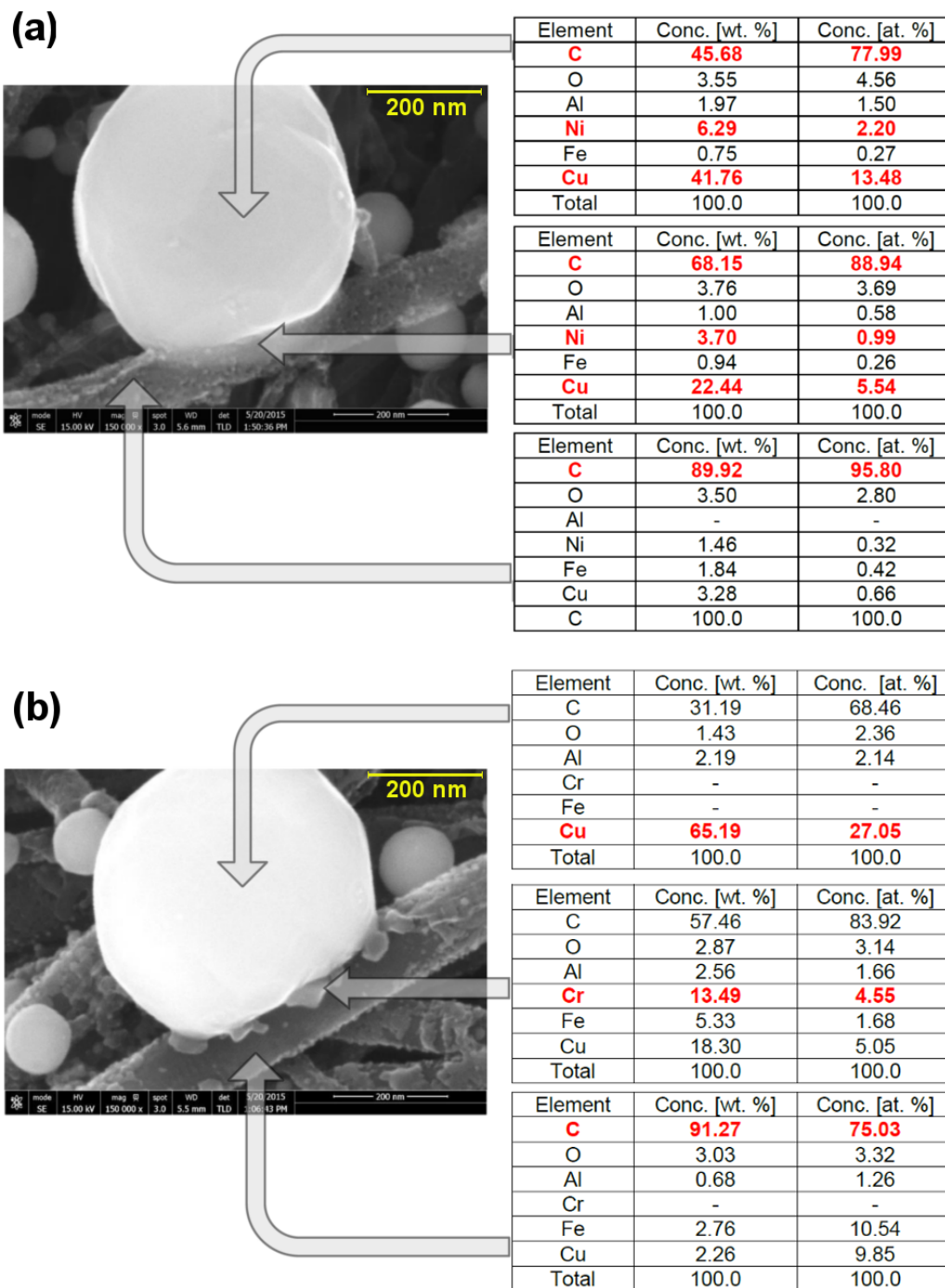


Figure S2: SEM images and EDX analysis of (a) Cu/Ni and (b) Cu/Cr sputtered on vertically aligned MWCNTs after vacuum heat-treatment of up to 800° C . The most important elements in each case are highlighted in red.

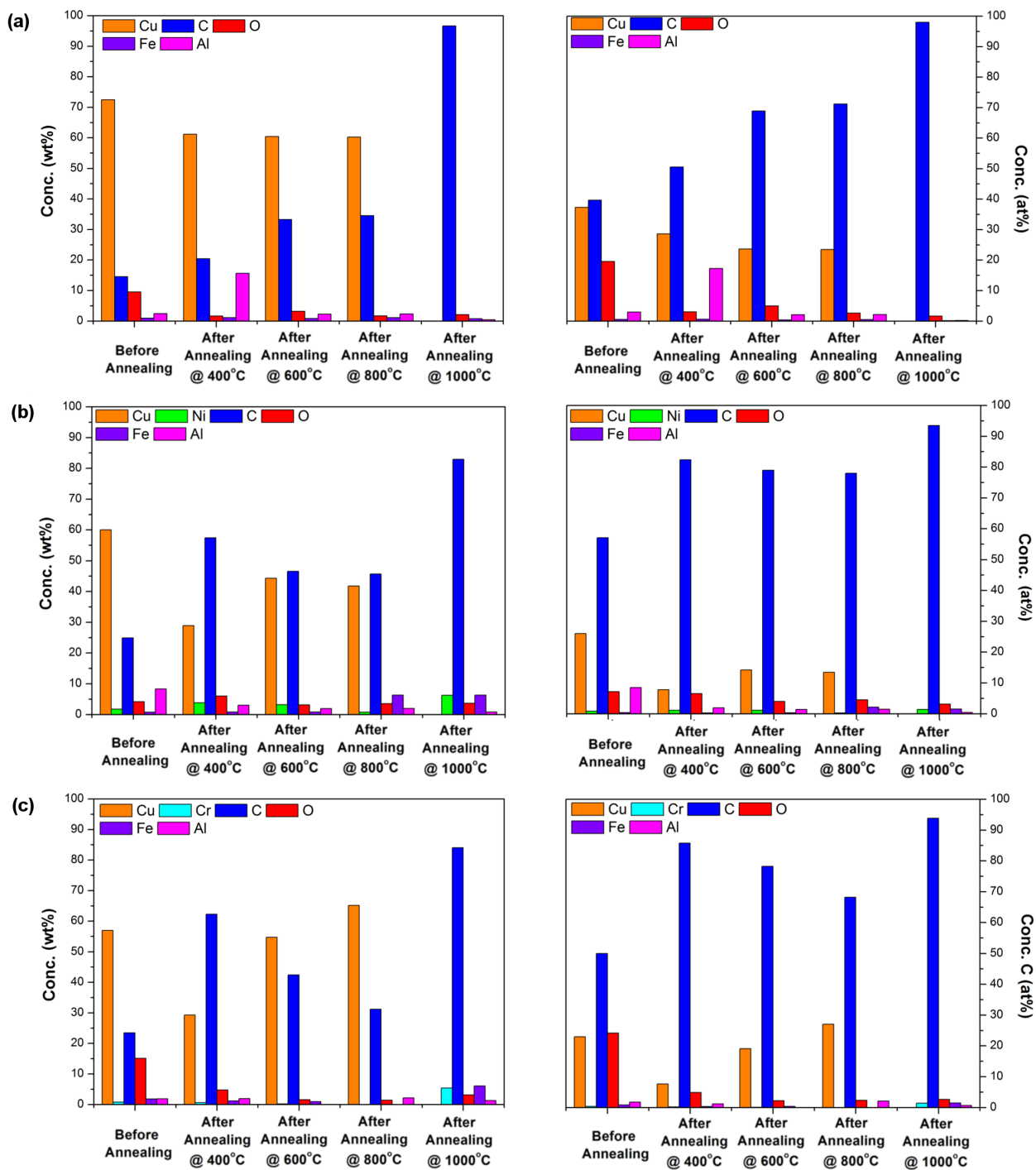


Figure S3: EDX analysis of (a) Cu, (b) Cu/Ni and (c) Cu/Cr sputtered on vertically aligned MWCNTs before and after vacuum heat-treatment of up to 400° C, 600° C, 800° C and 1000° C.

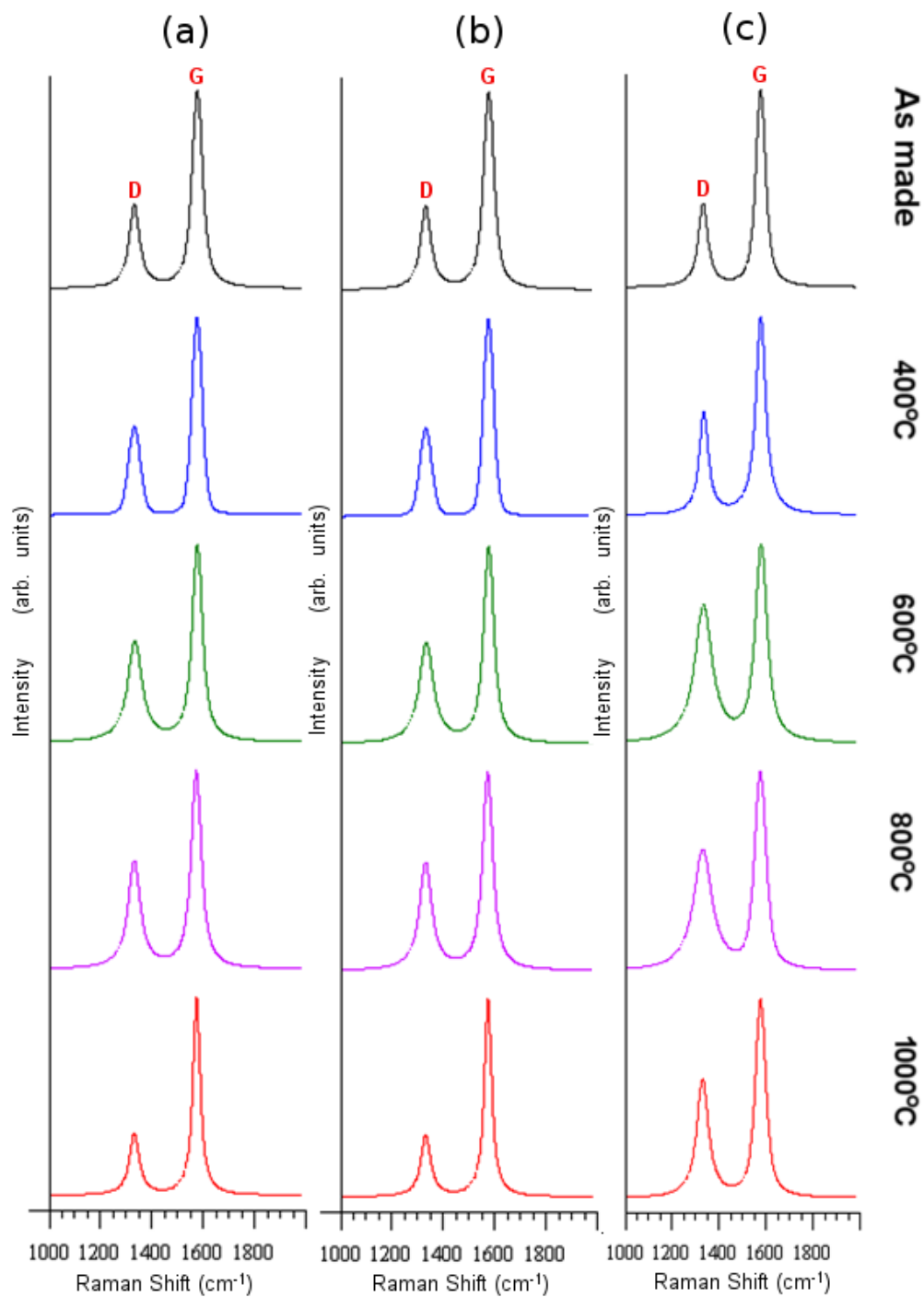


Figure S4: Raman spectra of (a) Cu, (b) Cu/Ni and (c) Cu/Cr sputtered on vertically aligned MWCNTs before and after vacuum heat-treatment of up to 400° C, 600° C, 800° C and 1000° C. D and G indicate the defect-induced and graphitic vibration bands respectively.

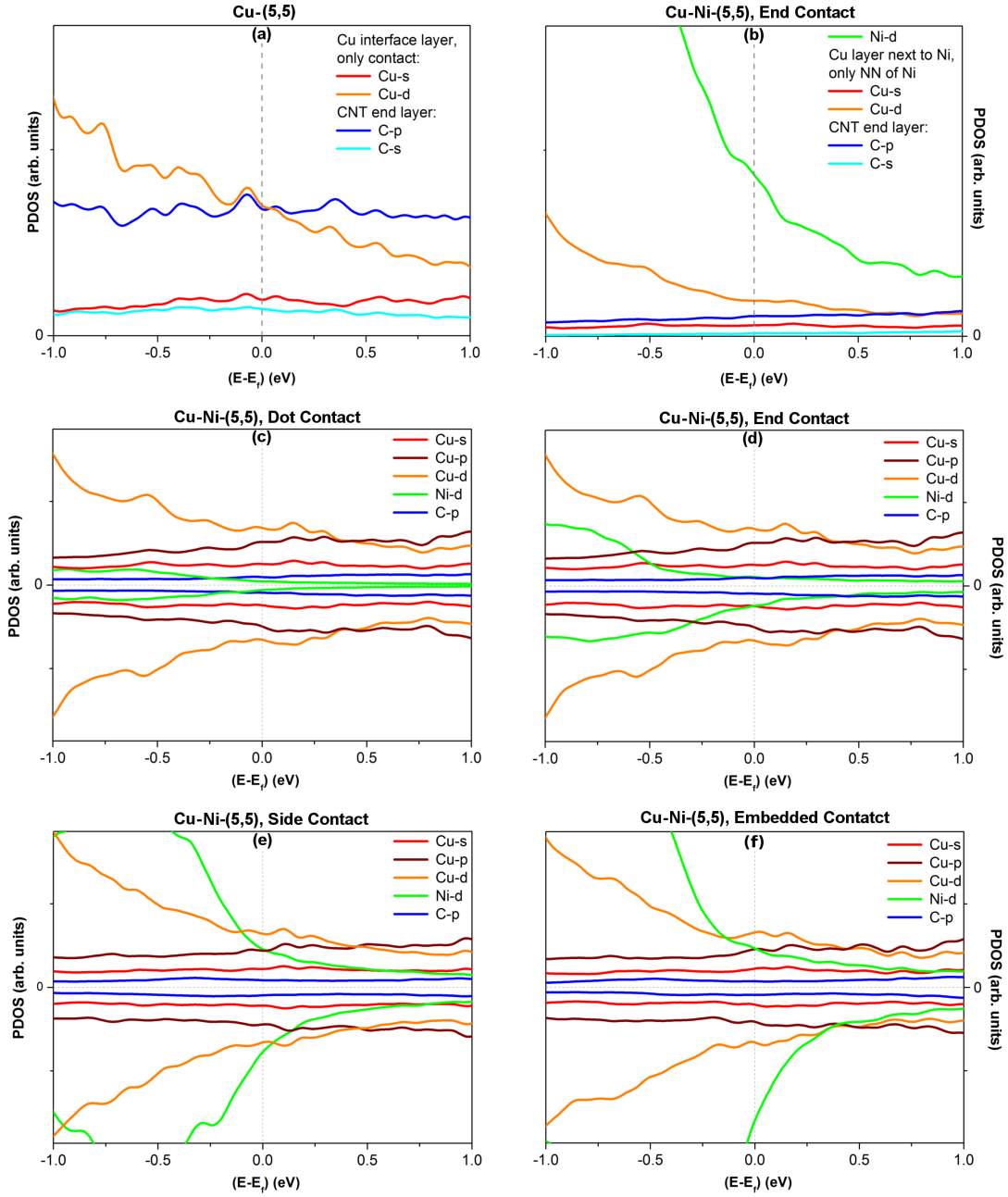


Figure S5: (a)-(b) Partial density of states (PDOS) of the metal-CNT interface areas of the Cu-(5,5) and Cu-Ni-(5,5) systems. (c)-(f) Spin resolved PDOS of the Cu-Ni-(5,5) systems with different contact types. The PDOS scale is the same in (c)-(f).  $E_F$  is the Fermi energy.

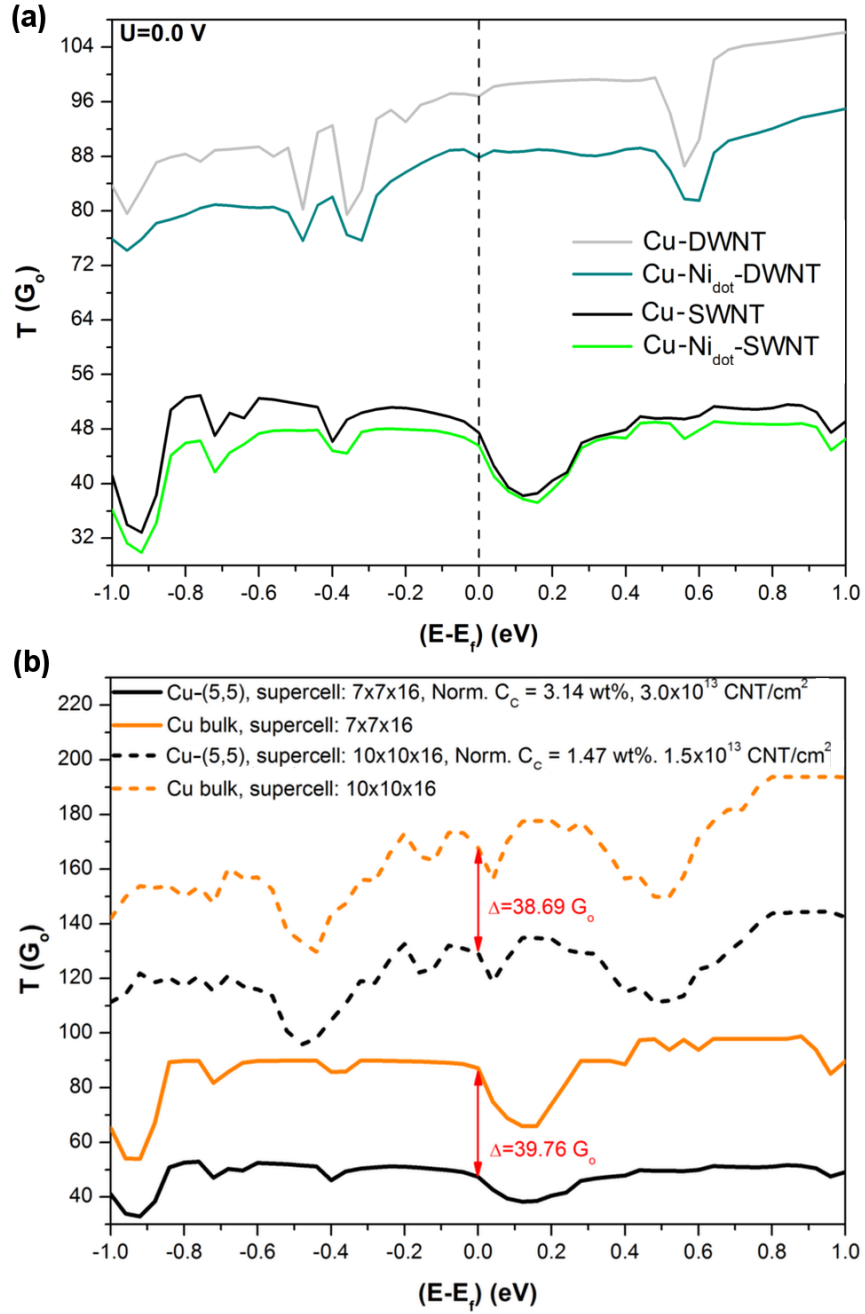


Figure S6: (a) Zero-bias transmission spectra for composites containing single and double walled CNTs (SWNT and DWNT) with and without an additional Ni-dot type contact. (b) Zero-bias transmission spectra for two Cu-CNT (5,5) composites with different CNT concentrations (CC). Results are compared to corresponding spectra for bulk Cu.  $E_F$  is the Fermi energy.

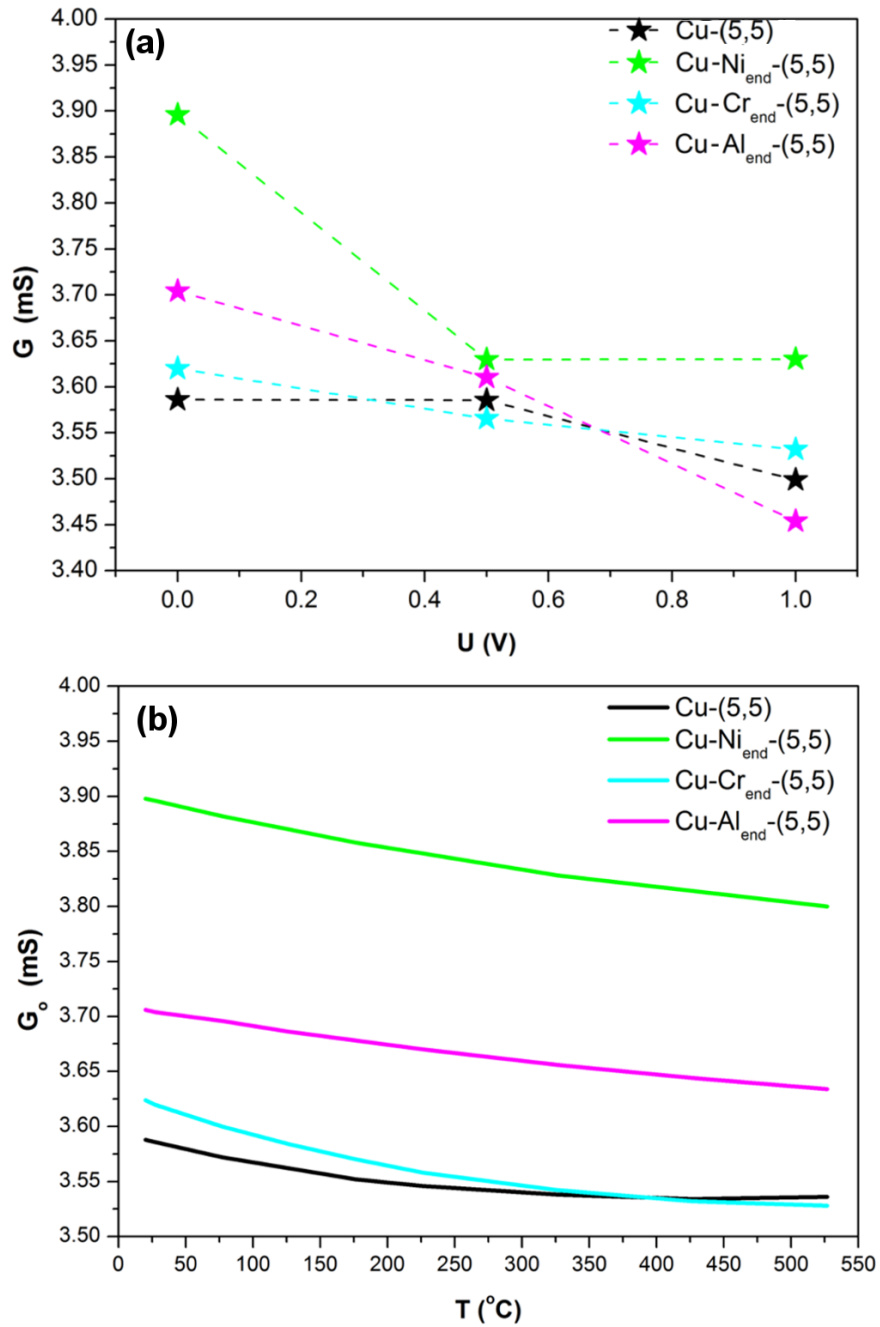


Figure S7: (a) The computed conductance as a function of applied voltage for Cu-M-(5,5) end type contact systems. (b) The temperature dependence of the conductance for the same end type contact systems.

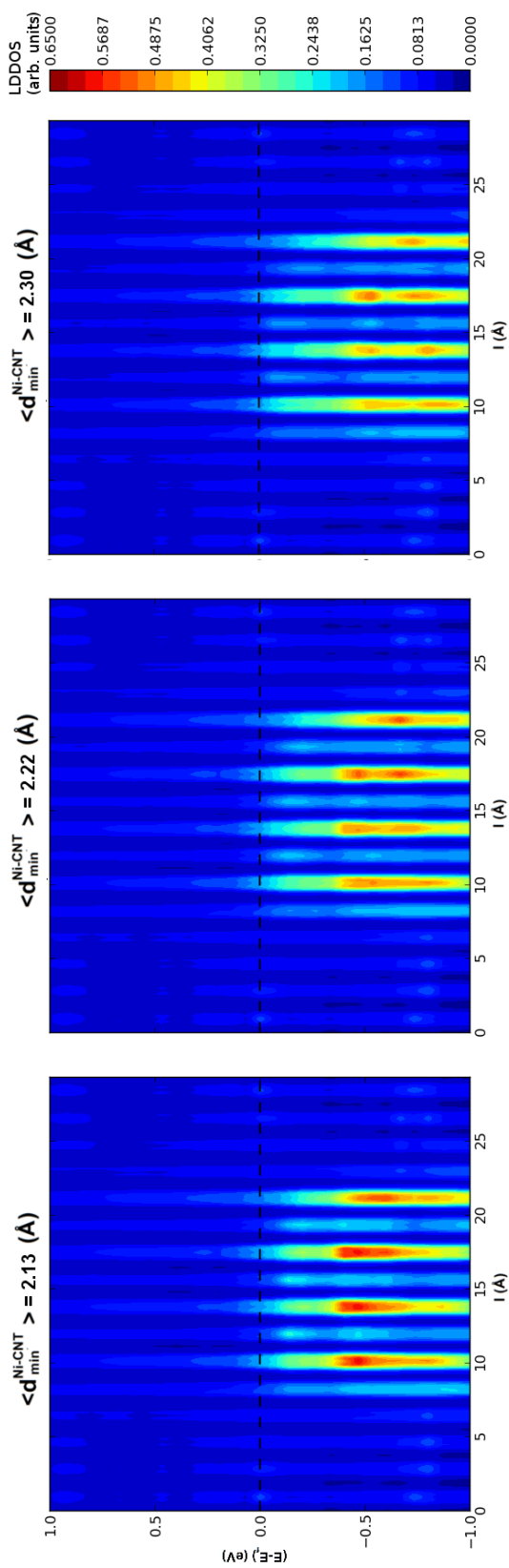


Figure S8: The energy resolved LDDOS of three different Cu-Ni-(5,5) side contact systems. Ni atoms around the lateral surface of the CNT were placed at different distances from the nanotube. Distance is calculated as an arithmetic mean of the minimal separation distance between C and Ni atoms. Systems were not optimized after replacing the first layer of surrounding Cu atoms with Ni atoms.

Table S1: Measured conductance of sputtered CNT tracks deposited on quartz plates before ( $G_i$ ) and after ( $G_f$ ) heat treatment. Samples were sputtered for 6 min at 80 mA and vacuum heated to 800° C without holding at the target temperature.

track	sputtered	sample	$G_i$ (mS)	$G_f$ (mS)	$\Delta G$ (%)
—	Ni	1	$< 10^{-5}$	0.058	—
		2		0.062	
		3		0.062	
	Cr	4	$< 10^{-5}$	0.003	—
		5		0.007	
		6		0.005	
CNT	—	7	2.212	3.082	39.32
		8	2.091	2.823	35.04
		9	2.215	2.917	31.71
	Cu	10	1.614	2.311	43.16
		11	1.983	2.861	44.29
		12	4.386	6.365	45.13
	Ni	13	4.394	9.950	126.47
		14	3.617	8.606	137.95
		15	1.676	3.453	105.97
	Cr	16	4.907	7.163	45.99
		17	4.371	6.452	47.61
		18	2.532	3.768	48.79

Table S2: Computed structural and electronic properties of two Cu-((5,5) carpet) systems with and without Ni doping: coefficients of variation of nanotube radius (CV), interfacial strengths  $\tau$ , matrix surface energies  $\gamma$ , and electrostatic potential barriers between the metal matrix and nanotube ( $\Delta\bar{V}_H$ ).

system	CV	$\tau$ (J/m <sup>2</sup> )	$\gamma$ (J/m <sup>2</sup> )	$\Delta\bar{V}_H^{left}$ (eV)	$\Delta\bar{V}_H^{right}$ (eV)
Cu-((5,5) carpet)	0.029	6.15	6.90	2.757	2.799
Cu-Ni-((5,5) carpet)	0.043	9.46	10.47	1.497	1.035

## References

- S1. Milowska, K. Z. Influence of Carboxylation on Structural and Mechanical Properties of Carbon Nanotubes: Composite Reinforcement and Toxicity Reduction Perspectives. *J. Phys. Chem. C* **2015**, *119*, 26734–26746.